Tellus (2002), 54B, 768–783

TELLUS
ISSN 0280–6509

Estimates of regional surface carbon dioxide exchange and carbon and oxygen isotope discrimination during photosynthesis from concentration profiles in the atmospheric boundary layer

By JULIE M. STYLES[1,2*], JON LLOYD[2], DANIIL ZOLOTOUKHINE[3], KIERAN A. LAWTON[2], NADJA TCHEBAKOVA[3], ROGER J. FRANCEY[4], ALMUT ARNETH[2,5], DIMA SALAMAKHO[3], OLAF KOLLE[2] and E.-DETLEF SCHULZE[2], [1]*CRC for Greenhouse Accounting and Environmental Biology Group, Research School of Biological Sciences, Institute of Advanced Studies, Australian National University, Canberra ACT 0200, Australia;* [2]*Max-Planck-Institut für Biogeochemie, Postfach 100164, Jena 07701, Germany;* [3]*V.N. Sukachev Forest Institute, Siberian Division, Russian Academy of Science, Akademgorodok, 660036 Krasnoyarsk, Russian Federation;* [4]*CSIRO Division of Atmospheric Research, Private Bag No.1, Aspendale, VIC 3195 Australia;* [5]*Landcare Research, Manaaki Whenua, PO Box 69, Lincoln, New Zealand*

(Manuscript received 9 July 2001; in final form 10 June 2002)

ABSTRACT

The integrating properties of the atmospheric boundary layer allow the influence of surface exchange processes on the atmosphere to be quantified and estimates of large-scale fluxes of trace gases and plant isotopic discrimination to be made. Five flights were undertaken over two days in and above the convective boundary layer (CBL) in a vegetated region in central Siberia. Vertical profiles of CO_2 and H_2O concentrations, temperature and pressure were obtained during each flight. Air flask samples were taken at various heights for carbon and oxygen isotopic analysis of CO_2. Two CBL budget methods were compared to estimate regional surface fluxes of CO_2 and plant isotopic discrimination against $^{13}CO_2$ and $C^{18}O^{16}O$. Flux estimates were compared to ground-based eddy covariance measurements. The fluxes obtained for CO_2 using the first method agreed to within 10% of fluxes measured in the forest at the study site by eddy covariance. Those obtained from the second method agreed to within 35% when a correction was applied for air loss out of the integrating column and for subsidence. The values for ^{13}C discrimination were within the range expected from knowledge of C_3 plant discriminations during photosynthesis, while the inferred ^{18}O discrimination varied considerably over the two-day period. This variation may in part be explained by the enrichment of chloroplast water during the day due to evaporation from an initial signature in the morning close to source water. Additional potential complications arising from the heterogeneous nature of the landscape are discussed.

1. Introduction

Concentrations of trace gases within the atmospheric boundary layer reflect exchange processes occurring at the surface over a regional scale (10^2–10^4 km^2). On days of high radiation load, low winds and clear skies, turbulence driven by thermal convection mixes air within the atmospheric boundary layer so that concentrations of scalar quantities such as CO_2 and its isotopes, H_2O and potential temperature are approximately constant with height. The influences of inhomogeneities at the surface are therefore smoothed in the atmosphere, and the signal present in the evolution of atmospheric concentrations through

*Corresponding author.
e-mail: julie.styles@oregonstate.edu
Current address: Department of Forest Science, Oregon State University, 321 Richardson Hall, Corvallis, Oregon 97331-5752, USA.

the day represents the weighted average surface flux over the region. Mixing within the convective boundary layer (CBL) occurs rapidly (∼15 min) relative to the time scale for substantial changes in surface fluxes (∼1 h except near sunrise and sunset). This allows simple mass-balance approaches to relate average CBL concentrations to surface flux magnitudes. These approaches are collectively called CBL budget methods, and may be partitioned into "differential" CBL methods and "integral" CBL methods according to whether or not the conservation equations are integrated in time before application (Raupach et al., 1992). The methods have been used successfully to model diurnal growth of the depth of the mixed layer and/or its scalar content (e.g. McNaughton and Spriggs, 1986; Denmead et al., 1996; Cleugh and Grimmond, 2001) and to infer average regional fluxes of sensible and latent heat and CO_2 from diurnal changes in corresponding scalar concentrations over both homogeneous and heterogeneous landscapes (e.g. Brutsaert and Mawdsley, 1976; Munley and Hipps, 1990; Raupach et al., 1992; Denmead et al., 1996; Cleugh and Grimmond, 2001).

The present study compares two budget methods for inferring surface CO_2 fluxes and carbon and oxygen isotope discrimination during CO_2 assimilation over a forest and bog region in central Siberia in July 1998. The integral CBL (ICBL) budget method was only recently for the first time applied to the carbon isotope composition of CO_2 to infer regional carbon isotope discrimination during photosynthesis (Lloyd et al., 1996; Lloyd et al., 2001). This study will be the first to additionally infer regional oxygen isotope discrimination. The two budget methods investigated here use similar scalar conservation considerations. Despite both effectively being ICBL methods, this label will be applied to the first method, which utilises the idealised properties of the CBL to find an analytical solution to the surface fluxes. The second method, referred to as the "height integration method", is more numerical in its approach, calculating the molar difference in the sampled air column over the integration period. It will be seen that the height integration method gives reasonable results only when corrections for subsidence are incorporated as for the ICBL method, as well as for column expansion or contraction (loss or gain of air mass). The comparison of the two budget approaches highlights strengths and weaknesses in both, and assesses the importance and validity of assumptions commonly adopted in CBL budget methods. The application of the methods to inference of plant isotope discrimination requires interpretation based on ecophysiological theory of CO_2 assimilation and isotopic fractionation during diffusion and fixation. Estimates of isotope discrimination obtained from atmospheric inversions such as presented here have the potential to reveal weaknesses in the simplified physiological models, showing when and to what degree additional complicating processes are important.

2. Theory

2.1. ICBL budget method

The height of the CBL grows during the day as thermal plumes overshoot the capping inversion and entrain overlying air into the CBL. A mass balance shows that the rate of change of scalar storage in the CBL is a function of the growth rate of the CBL, the vertical velocity at the top of the CBL, the scalar concentration of air being entrained and the surface scalar flux (e.g. Lloyd et al., 2001):

$$\frac{\mathrm{d}(M_\mathrm{B}c_\mathrm{B})}{\mathrm{d}t} = c_+\frac{\mathrm{d}M_\mathrm{B}}{\mathrm{d}t} + (c_\mathrm{B} - c_+)W_+ + F_c \tag{1}$$

where the subscripts B and + refer to the mean value within and that just above the boundary layer, respectively; $M_\mathrm{B} = \rho_\mathrm{B} h$ is the number of moles of air per unit ground area in the CBL, with ρ being the molar air density (mol m^{-3}) and h the height of the CBL (m); c is the scalar concentration (mol mol^{-1}); F_c is the surface flux of scalar c (mol m^{-2} s^{-1}); and $W_+ = \rho_+ w_+$ is the molar air flux per unit area into or out of the boundary layer due to the mean vertical velocity w_+ (m s^{-1}), defined as positive upwards. Here it is necessary that h be defined as the height just above the entrainment zone, so that a positive w_+ results in a loss of air at concentration c_+ through the top of the boundary layer, and a compensating gain of air at concentration c_B through the sides of the column of air under consideration. The reverse is true for a negative w_+ (subsidence). The vertical gradient in scalar concentration above the CBL is assumed to be zero, a reasonable assumption for CO_2 and its isotopes according to the data obtained in this study. An equivalent equation is derived in Raupach [2000, his eq. (A9)] as a special case of the conservation equation in a moving region with spatially variable fluid density.

Equation (1) can be integrated to relate mean conditions at two different times during the day to the average surface flux over that period to obtain the integral CBL (ICBL) budget equation (Lloyd et al., 2001):

$$\langle F_c \rangle = \frac{(c_{B1} - c_+)M_{B1} - (c_{B0} - c_+)M_{B0}}{T} - (\langle c_B \rangle - c_+)\langle W_+ \rangle \quad (2)$$

where angle brackets denote time averaging and T (s) is the integration period from time t_0 to t_1. The average of the product of quantities in the subsidence term is approximated by the product of their averages. In practice, the averages are estimated from the mean of values at consecutive sampling times.

In eq. (2) it is assumed that the scalar concentration above the boundary layer, c_+, is constant in time. Relaxing this assumption gives an additional contributing term:

$$\langle F_c \rangle = \frac{(c_{B1} - c_{+1})M_{B1} - (c_{B0} - c_{+0})M_{B0}}{T} - (\langle c_B \rangle - \langle c_+ \rangle)\langle W_+ \rangle + \frac{1}{T}\int_{t_0}^{t_1} M_B \frac{\mathrm{d}c_+}{\mathrm{d}t}\mathrm{d}t. \quad (3)$$

To evaluate the additional term [the last term in eq. (3)] we can approximate the integral by treating the terms within as independent and integrating each separately as was done for the subsidence term in eq. (2). This then leads to an equation identical to eq. (2) except that average free troposphere concentrations are used:

$$\langle F_c \rangle = \frac{(c_{B1} - \langle c_+ \rangle)M_{B1} - (c_{B0} - \langle c_+ \rangle)M_{B0}}{T} - (\langle c_B \rangle - \langle c_+ \rangle)\langle W_+ \rangle \quad (4)$$

where again the time average is calculated as the mean of values at consecutive sampling times, $\langle c_+ \rangle = (c_{+1} + c_{+0})/2$. If free tropospheric concentrations are assumed to be constant with height, then their variation with time implies that significant advection must be occurring. In this case one might expect that concentrations within the boundary layer may similarly be affected. Air flow above the boundary layer, however, is decoupled from that within, so that advection above does not necessarily imply advection within. In addition, since scalar concentrations in the free troposphere are also decoupled from surface influences and the air there is stable, horizontal heterogeneity above the boundary layer may be preserved for several days in the absence of large-scale synoptic events. In contrast, mixing within the boundary layer occurs over several minutes.

2.2. *Height integration method*

The second approach investigated here calculates total mass or moles of scalar per unit ground area up to an arbitrary height where conditions are assumed to be constant with time, here taken to 3000 m. This method was first applied by Wofsy et al. (1988) to infer regional CO_2 fluxes over the Amazon basin. The method does not require knowledge of h, but it requires the integrating region to extend high enough that vertical air flow is negligible or can be estimated and concentrations are invariant in both space and time. Differences in scalar molar density at different times can be equated to average surface flux over that period, so that:

$$\langle F_c \rangle = \frac{1}{T}\sum_i [(\rho_i c_i)_1 - (\rho_i c_i)_0]\,\Delta z_i \quad (5)$$

where $T = t_1 - t_0$ is the integration period; i represents the layer from z_{i-1} to z_i, and $\Delta z_i = z_i - z_{i-1}$. Note that eq. (5) can be applied with only two layers being chosen: within and above the CBL. With the assumption of time-invariant c_+, it then reduces to eq. (2) without the subsidence term, noting that the rate of change of moles of air per unit ground area in the CBL is equal to minus the rate of change of moles of air in the free troposphere, so that $M_{B1} - M_{B0} = -(M_{T1} - M_{T0})$, where $M_T = \bar{\rho}_T(3000 - h)$ is the moles of air per unit ground area in the free troposphere from h to 3000 m.

A change in the average density within the integrating column from one time to the next implies that air has been gained or lost through the top or sides of the column. The density profiles obtained in this study showed that as the temperature increased during the day the air density near the ground decreased, while that above the CBL tended to increase slightly. The average density throughout the column decreased during the day. Assuming that air was lost through the top of the column, this loss can be accounted for by including an additional term involving the difference in average density through the column over the day $\bar{\rho}_1 - \bar{\rho}_0$:

$$\langle F_c \rangle = \frac{1}{T}\left\{\sum_i [(\rho_i c_i)_1 - (\rho_i c_i)_0]\,\Delta z_i - (\bar{\rho}_1 - \bar{\rho}_0) z_R c_R\right\} \quad (6)$$

where z_R is the height to which the integration is taken and c_R is the scalar concentration at that height. A term can also be included to account for air flow through the top of the column that is compensated by horizontal flow (i.e. subsidence) as in eq. (4) to obtain:

$$\langle F_c \rangle = \frac{1}{T}\left\{ \sum_i [(\rho_i c_i)_1 - (\rho_i c_i)_0]\,\Delta z_i - (\bar{\rho}_1 - \bar{\rho}_0) z_R c_R \right\} + \langle W_+ \rangle (\langle c_+ \rangle - \langle c_B \rangle) \quad (7)$$

where the subsidence correction requires average concentrations within and above the CBL to be determined as in the integral budget method of eq. (4).

2.3. Application to isotopes of CO_2

Equations (4)–(7) can be applied to any scalar, including an isotope of a particular species. Isotopic discrimination can then be calculated from application of these equations to both the scalar and its "iso-concentration" (isotopic composition times concentration, δc). Isotopic composition is defined as $\delta = (\mathcal{R}/\mathcal{R}_{\mathrm{std}}) - 1$, where $\mathcal{R} = c^*/c$ is the ratio of concentration of minor to major isotope of scalar c, with the asterisk indicating the minor isotope, and $\mathcal{R}_{\mathrm{std}}$ is that for an isotopic standard of the same species. The flux of minor isotope is then given by $F_{c*} = \mathcal{R}_{\mathrm{std}}(F_{\delta c} + F_c)$, where the product δc is treated the same as any other scalar, and the isotopic composition of the scalar flux is given by $\delta_{F_c} = (F_{c*}/F_c/\mathcal{R}_{\mathrm{std}}) - 1$. In the case of carbon dioxide,

$$\delta_{F_{\mathrm{CO_2}}} = \frac{A\delta_A + R\delta_R}{A + R},$$

where A is the net assimilation flux of CO_2 which includes leaf respiration, R is the combined root, soil and stem respiration flux, and δ_A and δ_R are the isotopic compositions of these fluxes. The sign convention adopted here is positive upwards, so that A is negative during the day as plants assimilate CO_2. Isotopic discrimination during assimilation, defined as

$$\Delta_A = \frac{\mathcal{R}_\mathrm{B}}{\mathcal{R}_\mathrm{A}} - 1 \approx \delta_\mathrm{B} - \delta_\mathrm{A},$$

where the subscripts B and A refer again to ambient (within CBL) air and air carried by the assimilation flux, is then given by:

$$\Delta_\mathrm{A} = \delta_\mathrm{B} - \frac{F_{\delta c} - R\delta_R}{F_c - R}. \quad (8)$$

2.4. Modelling isotope discrimination during CO_2 assimilation

Physiological models of carbon and oxygen isotope discrimination were used to interpret the estimates obtained by the CBL budget methods.

Carbon and oxygen isotopic composition of CO_2 is expressed on the PDB-CO_2 scale (relative to CO_2 derived from the Pee-Dee Belemnite calcite formation) and oxygen isotope composition of water on the SMOW scale (relative to Standard Mean Ocean Water). These scales are now strictly called VPDB-CO_2 and VSMOW, respectively, to reflect standardisation protocol penned at the International Atomic Energy Agency in Vienna, 1995, but the V prefix will be omitted in this paper.

2.4.1. Carbon isotope discrimination. The simplest model for carbon isotope discrimination during plant uptake of CO_2 is given by $\Delta^{13}C = a + (b - a)c_\mathrm{i}/c_\mathrm{a}$ (Farquhar et al., 1982), where a is the fractionation occurring due to diffusion in air (calculated as 4.4‰), b is the effective net fractionation during carboxylation (measured as ~27‰), and c_i and c_a are the intercellular and ambient partial pressures of CO_2, respectively. Estimates of carbon isotope discrimination and its diurnal or day to day variation therefore describe variation in intercellular CO_2 concentration with respect to ambient concentration.

2.4.2. Oxygen isotope discrimination. CO_2 entering the chloroplast equilibrates with water there, and exchange of oxygen atoms is catalysed by the enzyme carbonic anhydrase. Some of the CO_2 is assimilated, but some diffuses back out of the leaf, carrying the isotopic signature of chloroplast water. Chloroplast water is enriched in heavy isotopes compared to source water because lighter isotopes are preferentially evaporated (Farquhar et al., 1989).

Isotopic composition of water at the sites of evaporation within the leaf, δ_e, is modelled by $\delta_\mathrm{e} = \delta_\mathrm{s} + \varepsilon_\mathrm{k} + \varepsilon^* + (\delta_\mathrm{v} - \delta_\mathrm{s} - \varepsilon_\mathrm{k})e_\mathrm{a}/e_\mathrm{i}$, where δ_s is the oxygen isotopic composition of source water, δ_v is that of water vapour in the surrounding air, ε_k is the kinetic fractionation factor (28.5‰ through the stomata and 18.9‰ in the boundary layer and the effective fractionation is here taken as 26‰), ε^* is the proportional depression of equilibrium vapour pressure by the heavier molecule (9.2‰ at 25 °C), and e_a and e_i are the vapour pressures in the ambient air and intercellular spaces, respectively. This equation was developed by Craig and Gordon (1965) for a free water surface and modified by Farquhar et al. (1989) for application to the leaf, and is referred to as the Craig–Gordon model.

In analogy with the carbon case, oxygen isotope discrimination is modelled by $\Delta^{18}O = a_k + (\delta_c - \delta_a)c_c/(c_a - c_c)$ (Farquhar and Lloyd 1993), where a_k is the weighted mean fractionation during diffusion to the sites of carboxylation (taken as 7.4‰); c_c and c_a are the partial pressures of CO_2 in the chloroplast and ambient air, respectively; and δ_c and δ_a are the oxygen isotope composition of CO_2 in the chloroplast and ambient air, respectively. CO_2 is assumed to be in equilibrium with chloroplast water before fixation, and the isotopic composition of the latter is approximated by δ_e. Fractionation during equilibration is 41.2‰ at 25 °C (O'Neill et al., 1975: this is close to the difference between the PDB-CO_2 and SMOW scales of 41.47‰).

3. Methods

Profiles of CO_2 concentration, temperature, humidity and pressure were obtained in and above the convective boundary layer at a remote field site in central Siberia near the town of Zotino, at 60.6°N, 89.4°E. Flask samples of air were taken for isotopic analysis of CO_2. Two flights were made on 23 July 1998 at 1400 h and 2100 h, and three on 24 July 1998 at 0730 h, 1400 h and 1900 h (all times are local standard times, UTC+7).

Surface fluxes were measured from towers on the ground by the eddy covariance technique at two sites reflecting the two dominant ecosystem types in the area: forest and bog. NDVI data for the region suggest that the ratio of forest to bog area is about 5 (Lloyd et al., 2001). The ground-based measurements at the bog site are described in detail in Arneth et al. (2002) and Kurbatova et al. (2002), and those at the forest site are described in Tchebakova et al. (2002), Lloyd et al. (2002a) and Shibistova et al. (2002). These measurements cannot be considered to be representative of the entire region sampled by the CBL budget methods, but give an indication of the magnitude of fluxes to be expected from the two major ecosystem types in the region.

Atmospheric sampling protocol and corrections to raw data were the same as reported in Lloyd et al. (2002b), with the main points being described here. CO_2 concentration within the atmospheric boundary layer was measured with a Li-Cor 6251 infra-red gas analyser (IRGA) operated in absolute mode, temperature and humidity were measured with a Vaisala HMP35D capacitive humidity sensor and PT100 platinum resistance sensor, and pressure with a Vaisala PTB101B aneroid barometer. Output was logged at 1 Hz frequency on a Delta T DL3000 datalogger. An Antonov AN2 plane was used with air intake and temperature/humidity sensor attached to the port wing. The engine exhaust was located on the starboard wing. Flask samples of air were obtained with a system based on that used by the Global Atmospheric Sampling Laboratory (GASLAB), CSIRO Atmospheric Research, Australia. One-litre flasks had been preconditioned by heating and flushing with nitrogen. During sampling flasks were flushed for 4 min with dry air (passed through a magnesium perchlorate trap) at ambient pressure then pressurised to 2 bar absolute pressure and analysed at GASLAB for concentrations of CO_2 and carbon and oxygen isotopic composition of CO_2.

During each flight profiles were obtained over both a forest-dominated area (*Pinus sylvestris* with moss and lichen ground cover) and a bog-dominated area (*Sphagnum* and *Carex* species, *Scheuchzeria palustris* and *Andromeda polifolia*). Sampling of CO_2 concentration, temperature and pressure would begin 50–100 m above the ground and run continuously with flask sampling at intervals while ascending to 3000 m in a spiral of ~2 km radius. A similar descending spiral would then be made over the second sampling area. Typically six to eight flasks were filled during each profile, generally at heights around 50–100, 200, 500, 1000, 1500, 2000, 2500 and 3000 m for both the ascent and descent. Zero and span on the IRGA were adjusted at the start of each flight using nitrogen and two reference CO_2 gases at 340 and 380 ppm, respectively. Reference gas was also run through the IRGA during each flask-sampling period for later correction of any drift. The correction was applied by interpolating the offset of reference values and subtracting this offset from the sample concentrations. This calibration also accounted for any pressure correction required in addition to the standard correction applied according to the Li-Cor software. Each ascent and descent typically took about half an hour to complete. Comparison of the two profiles obtained during each flight showed no discernable change in concentrations during the flight, indicating that the profiles could be treated as approximately instantaneous. Since the ascent and descent profiles corresponding to forest and bog areas were generally indistinguishable (see Discussion), the profile pairs were averaged and the times nominated for averaged profiles were roughly the median times for each pair.

Virtual potential temperature was calculated from measured temperature, pressure and humidity. Height was calculated from pressure data using the hydrostatic equation to obtain:

$$z = \frac{T_0}{\gamma}\left[1 - \left(\frac{p}{p_0}\right)^{\frac{R_m \gamma}{g}}\right]$$

where p is the pressure at height z; p_0 is that at the ground; T_0 is the virtual temperature at the ground; γ is the adiabatic lapse rate; R_m is the gas constant for dry air; and g is the acceleration due to gravity.

To reduce scatter due to horizontal inhomogeneity, average [CO_2], [H_2O], virtual potential temperature and air density were calculated for each 50-m interval up to 3000 m. The height of the boundary layer was estimated from the CO_2 and water vapour concentration jumps and level of the temperature inversion.

4. Results

4.1. Meteorological conditions

Mean sea level pressure obtained from the National Centers for Environment Prediction (NCEP) Reanalysis Project showed that a large high-pressure region was present to the north of the study site and this was fairly stable during the study period (Fig. 1). Individual flight trajectories carried out as described in Lloyd et al. (2002b) showed the prevailing winds for all flights in this study originated from a northerly direction.

Model data provided by NCEP for the 60°N, 90°E grid point (within ~70 km of the study site) suggested mean vertical velocities above the CBL of -0.001 m s^{-1} on the afternoon of 23 July and night of 23–24 July, -0.004 m s^{-1} in the morning of 24 July and -0.005 m s^{-1} on the afternoon of 24 July. The sign convention is positive upwards, so these velocities imply subsidence of the CBL. Mean vertical velocity at the top of the CBL could also be estimated from the drop in height overnight of the top of the CBL, as seen by the height of the residual layer. The velocity thus found, -0.008 m s^{-1}, was considerably larger than the NCEP model estimates. Since the value of -0.008 m s^{-1} was found from observed data and the comparison of the NCEP model estimates for the corresponding period was not good, this value was used for the entire study period, from mid-afternoon on 23 July to the evening of 24 July. Extrapolation of the estimated subsidence velocity to the previous and next day may be justified to some extent by the stable synoptic conditions present over the region (Fig. 1). The contribution of this term to the inferred assimilation flux for each integration period was around -1.8 μmol m^{-2} s^{-1}.

4.2. Observations of carbon dioxide concentrations and isotopic composition

Profiles of CO_2 and its carbon and oxygen isotopic composition on the afternoon and evening of 23 July show vertical structure typical of a well mixed atmospheric boundary layer, with concentrations fairly constant within and a sharp jump at its top (Figs. 2a, 3a and 4a). Average CBL CO_2 concentration in the afternoon was less than that in the evening because although net surface uptake was occurring, the boundary layer grew considerably in the intervening period, entraining free tropospheric air of much higher concentration (Fig. 2a). This pattern was also present in the $\delta^{13}C$ profiles, where the surface discrimination was positive but the carbon isotope composition of CO_2 in the CBL decreased in the evening due to entrainment of CO_2 of lighter carbon isotope composition (Fig. 3a). The oxygen isotope composition, however, increased significantly in the evening of 23 July due to the combined effects of entrainment of heavier (in oxygen isotopes) CO_2 and positive surface discrimination during that period (Fig. 4a).

The morning profiles on 24 July show very high CO_2 concentrations and low carbon and oxygen isotope composition in the nocturnal boundary layer (NBL) up to about 100 m (Figs. 2b , 3b and 4b). The residual layer concentrations in the morning and CBL concentrations in the afternoon and evening are very similar, and very little variation in boundary layer depth is observed (Fig. 2b). This is also evident in the carbon and oxygen isotope profiles (Figs. 3b and 4b). The profiles on this day do not allow immediate inferences to be drawn about the sign of the surface exchange, except for the obvious influence of respiration overnight with its lighter isotopic composition.

The morning flight on 24 July indicated the presence of a residual layer representing the previous day's CBL. The data for this flight were treated in two different ways. Firstly, residual layer concentrations were used in place of mixed layer concentrations in eq. (4). The NBL was ignored, with its influence accounted for only by its effect on measured concentrations in the

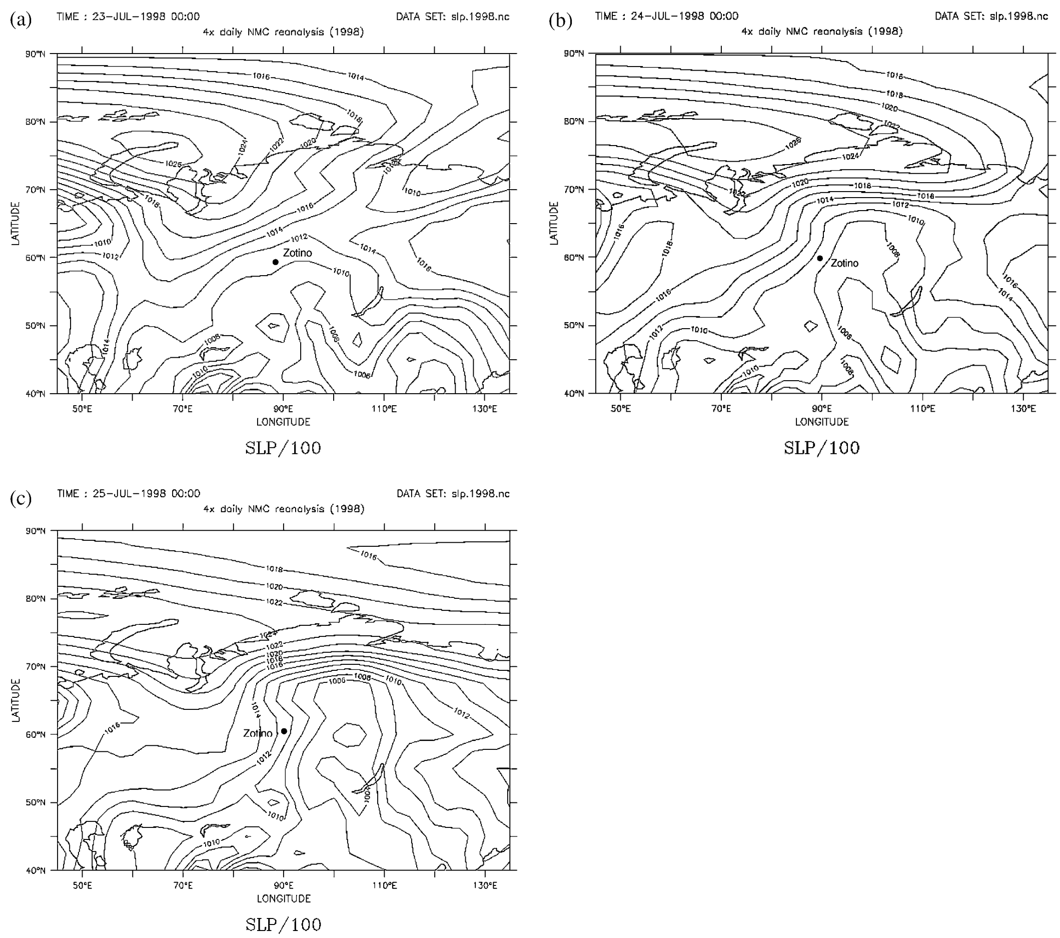

Fig. 1. Mean sea level air pressure surrounding the study region during the experiment, on (a) 23 July 1998 at 00:00 UTC (0700 h local time); (b) 24 July 1998 at 00:00 UTC (0700 h local time); and (c) 25 July at 00:00 UTC (0700 h local time). The nearest town to the study region, Zotino, is marked on the maps at 60.6°N, 89.4°E.

afternoon. The residual layer of the morning profile represented the state of the mixed layer the previous day when the vegetated surface became a net sink for sensible heat, thermal convection halted, and net ecosystem exchange became positive (at around 2100 h according to the eddy covariance measurements of heat and CO_2 flux). The afternoon profile showed the change in mixed layer concentration due to development of the new CBL including mixing in of the NBL and entrainment of the residual layer, as well as the influences of surface exchange occurring in the period between the two flights and subsidence. Based on the sharp concentration gradient at around 100 m height, it was assumed that at the time of the morning flight NBL concentrations had not mixed into the residual layer at all. The flux calculated from the 0730 h and 1400 h flights on 24 July by the ICBL method in this case represented average surface flux overnight (locked up in the NBL) plus flux in the morning period between flights, with a total integrating time of 17 h.

Secondly, surface flux for the morning period on 24 July (from 0730 h to 1400 h) could also be calculated treating the NBL as the mixed layer. Here residual layer concentrations were used for air entrained during CBL growth, but entrainment due to the mean vertical velocity was assumed to carry tropospheric concentration. A possible source of error with this interpretation is that it is assumed that entrainment stops

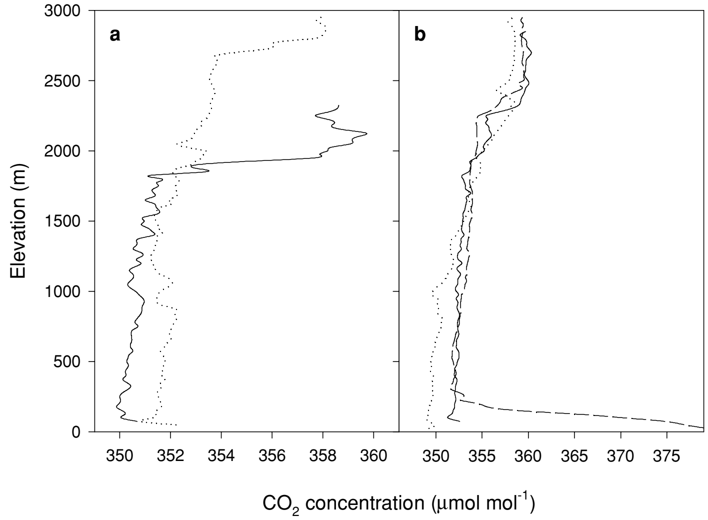

Fig. 2. Profiles of CO_2 concentration on (a) 23 July 1998 and (b) 24 July 1998. Concentration was monitored continuously and averaged over each 50-m height interval. Solid line is the afternoon profile (1400 h on each day), dotted line is the evening profile (2100 h on 23 July, 1900 h on 24 July) and dashed line is the morning profile (0730 h on 24 July).

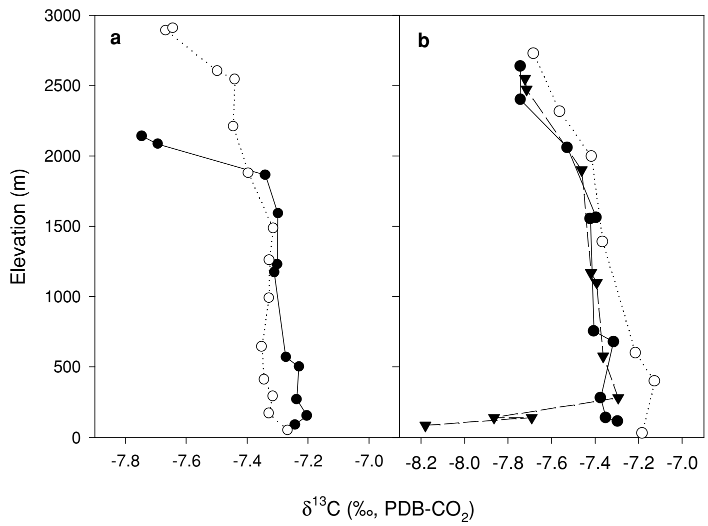

Fig. 3. Profiles of $\delta^{13}C$ on (a) 23 July 1998 and (b) 24 July 1998. Symbols indicate where flask samples were taken. Solid line with filled circles is the afternoon profile (1400 h on each day), dotted line with open circles is the evening profile (2100 h on 23 July, 1900 h on 24 July) and dashed line with filled triangles is the morning profile (0730 h on 24 July).

as soon as the entire residual layer has been incorporated. Residual layer entrainment usually occurs very quickly in the morning (Stull 1988), so that further CBL growth would require entrainment of free tropospheric air. Neglect of this contribution would tend to an underestimate of surface CO_2 uptake, but since CBL growth is much slower once the residual layer has been assimilated and the stable free tropospheric air is reached, this contribution should be small.

Boundary layer heights and average CO_2 concentration and isotopic composition within and above the CBL used in the budget methods are shown in

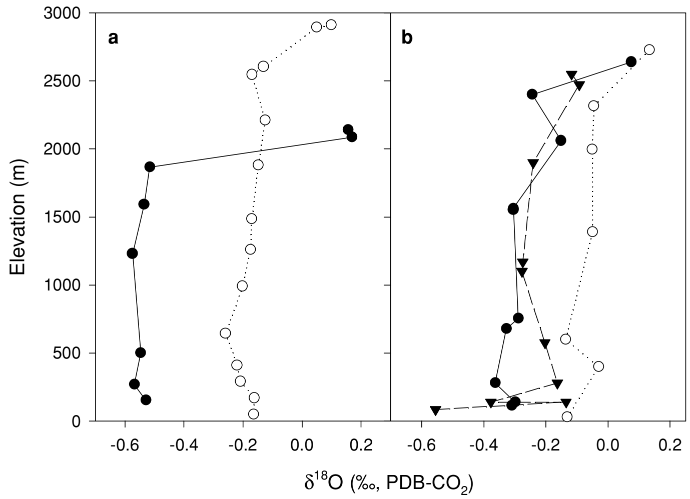

Fig. 4. Profiles of δ^{18}O on (a) 23 July 1998 and (b) 24 July 1998. Symbols indicate where flask samples were taken. Solid line with filled circles is the afternoon profile (1400 h on each day), dotted line with open circles is the evening profile (2100 h on 23 July, 1900 h on 24 July) and dashed line with filled triangles is the morning profile (0730 h on 24 July).

Table 1. Regional respiration was assigned as that measured by eddy covariance at the forest site (Lloyd et al., 2002a). Data were screened for low friction velocity and a respiration model was used for interpolation as described in Shibistova et al. (2002). Respiration rates for the four integration periods were thus found to be 2.85, 2.77, 2.37 and 2.52 μmol m^{-2} s^{-1}, respectively, for the periods PM 23 July, night + AM 23–24 July, AM 24 July and PM 24 July. Carbon isotopic composition of respired CO_2 was estimated to be constant at –26‰ (PDB-CO_2) from regression of night-time δ^{13}C versus inverse CO_2 concentration in the forest (Keeling, 1958; 1961, regression had the equation $y = 6700x - 26, r^2 = 1.00$). Oxygen isotopic composition of respired CO_2 was estimated as −15‰ (PDB-CO_2) from rainwater composition minus fractionation during equilibration with soil water (41.2‰ at 25 °C) and diffusion through the soil (−7.2‰, Miller et al., 1999). Oxygen isotope composition of recent rainwater was measured as −8‰ (SMOW).

Table 1. *Boundary layer height* (h)*,* CO_2 *concentrations* (C) *and carbon and oxygen isotopic composition (*δ^{13}*C and* δ^{18}*O) within (subscript B) and above (subscript +) the convective boundary layer measured for each flight*[a]

Flight time	1400 h 23 July 1998	2100 h 23 July 1998	0730 h 24 July 1998	1400 h 24 July 1998	1900 h 24 July 1998
h (m)	1850	2650	2350	2300	2150
C_N (μmol mol^{-1})			377.8		
C_B (μmol mol^{-1})	350.7	352.1	353.3	353.0	351.5
C_+ (μmol mol^{-1})	358.6	357.9	359.4	359.7	358.4
$\delta^{13}C_N$ (‰)			−8.02		
$\delta^{13}C_B$ (‰)	−7.27	−7.36	−7.38	−7.37	−7.26
$\delta^{13}C_+$ (‰)	−7.72	−7.66	−7.72	−7.74	−7.62
$\delta^{18}O_N$ (‰)			−0.47		
$\delta^{18}O_B$ (‰)	−0.70	−0.18	−0.25	−0.31	−0.08
$\delta^{18}O_+$ (‰)	0.16	0.07	−0.11	−0.08	0.04

[a]Values for the nocturnal boundary layer (subscript *N*, estimated height 100 m) in the morning of 24 July 1998 are also shown, and the subscript B for this flight refers to the residual layer.

Regression of oxygen isotope composition with inverse CO_2 concentration using the few flask samples obtained within the NBL also suggested a respired CO_2 oxygen isotope composition of −15‰.

4.3. *Estimation of regional CO_2 fluxes and isotopic discrimination*

The height integration method was applied using eqs. (5)–(7) to show the effect of the density and subsidence corrections to the method, with 50-m height intervals up to 3000 m (referred to as "height integration, $\Delta z = 50$"). The method was also applied using eq. (7) with only two integration layers representing within and above CBL concentrations for the two sampling times (referred to as "height integration, two-layer"). For the morning profile on 24 July three layers were required, representing the NBL, residual layer and free troposphere. An estimate of overnight and morning flux could also be obtained by this method in the same manner as for the ICBL method, by extending the residual layer and its average concentration to the ground as it would have been the previous evening.

CO_2 flux and isotopic discrimination were calculated for the afternoon of 23 July, overnight and morning of 23–24 July, morning of 24 July and afternoon of 24 July using both the integral CBL budget equation and the height integration method (Tables 2 and 3). Also shown in Table 2 are comparisons of the height integration method with and without correction for air loss due to column expansion (ρ correction) and for subsidence (w_+ correction). Reasonable agreement was found between flux and discrimination estimates by the two methods when ρ and w_+ corrections were applied, although the CO_2 flux estimates differ by 40% for the afternoon period of 24 July. Eddy covariance measurements of CO_2 flux from the forest and bog towers were averaged over each integrating period for comparison with the CBL budget estimates. Table 2 shows that CO_2 flux estimates by the ICBL method agree well with the eddy covariance measurements in the forest. Diurnal variation in CO_2 flux is shown by the half hour averages measured by eddy covariance at the two sites in Fig. 5, along with the CBL budget estimates by the two methods.

5. Discussion

5.1. *Carbon dioxide fluxes*

The CBL budget methods are very sensitive to measurement errors, since the flux that is sought is often the small difference between large terms. In particular, a significant subsidence term can change the sign of the inferred flux. Despite this, the flux estimates obtained by the ICBL budget method agreed very well with eddy covariance measurements made over the forest site (within 10%). Eddy covariance measurements over the bog site were considerably lower (Table 2,

Table 2. *CO_2 flux calculated from the integral CBL budget and height integration methods, and measured by eddy covariance*[a]

	CO_2 flux (μmol m^{-2} s^{-1})			
Integration period	PM 23 Jul	Night + AM 23–24 Jul	AM 24 Jul	PM 24 Jul
ICBL budget equation [eq. (4)]	−4.1	−1.9	−7.2	−6.6
ICBL budget equation using flask data [eq. (4)]	−3.9	−2.1	−6.1	−7.3
Height integration: $\Delta z = 50$ m [eq. (5)]	−5.8		−3.6	−13.5
Height integration: $\Delta z = 50$ m with ρ correction [eq. (6)]	−2.8		−3.4	−7.6
Height integration: $\Delta z = 50$ m with ρ and w_+ correction [eq. (7)]	−4.7		−5.1	−9.4
Height integration: 2-layer with ρ and w_+ correction [eq. (7)]	−4.8	−1.8	−6.1	−8.5
Eddy covariance: Forest tower	−4.1	−1.8	−6.9	−7.0
Eddy covariance: Bog tower	−2.6	−1.7	−3.6	−4.2

[a]Except for the second row, results are obtained using IRGA CO_2 concentration data.

Table 3. *Carbon and oxygen isotopic discrimination calculated from the integral CBL budget and height integration methods*[a]

Integration period	Δ_A (‰)			
	PM 23 Jul	Night + AM 23–24 Jul	AM 24 Jul	PM 24 Jul
ICBL budget equation $\Delta^{13}C$ [eq. (4)]	19.0	18.1	17.2	21.8
Height integration: 2-layer with ρ and w_+ correction g$\Delta^{13}C$ [eq. (7)]	19.9	18.0	17.7	22.9
ICBL budget equation $\Delta^{18}O$ [eq. (4)]	37	−1	−5	43
Height integration: 2-layer with ρ and w_+ correction $\Delta^{18}O$ [eq. (7)]	48	0	−4	40

[a]The CO_2 flux estimates required for the calculations were those obtained from the flask data using the same method as for the isotope calculations.

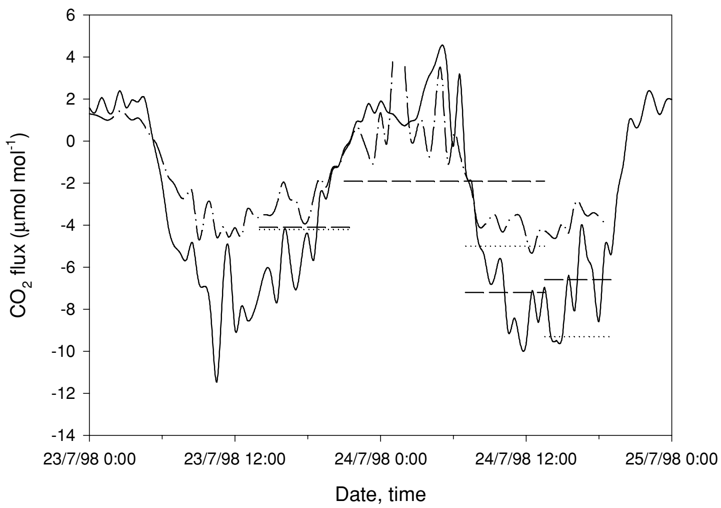

Fig. 5. Measured and modelled CO_2 flux, 23–24 July 1998. Solid line is the eddy covariance flux measurements over the forest; dash-dot line those over the bog; dashed lines are the ICBL budget method estimates; and dotted lines are the multilayer height integration method estimates with density and subsidence correction.

Fig. 5). No significant difference was found between CBL concentration profiles measured over forest and bog regions with one exception, indicating that the turbulent mixing in the CBL had likely smoothed the two influences. The exception was the afternoon profile of $\delta^{18}O$ on 23 July, in which oxygen isotope composition for the bog profile was depleted by around 0.2‰ (not shown). Methane concentrations were also higher for this profile (not shown). These data were not used in the analysis, and it seems likely that except for this case the profiles were dominantly influenced by forest exchange processes. In general, flux estimates from ICBL methods have source footprints of about 1000 km^2 under typical conditions (Cleugh and Grimmond 2001). This is in the order of the scale of heterogeneity of the landscape of this study, so it was somewhat surprising that the observations implied mixing was occurring over a larger scale.

CO_2 flux estimates obtained by the height integration method were reasonably close to eddy covariance measurements in the forest (within 35%) when the corrections for air loss and subsidence were applied. Without these corrections values were unsystematically and considerably different from measurements (Table 2). The estimates obtained using only two layers in the integration (within and above the CBL) were similar to those obtained with the full integration (Table 2). This allowed the height integration method to be used for isotopes, where continuous data were unavailable. To investigate the effect of having only few concentration data at discrete heights as in the isotopic calculations, flux estimates for CO_2 were calculated by the ICBL method using only concentrations obtained from flask analysis (Table 2). Values thus found were also in reasonable agreement with the forest surface measurements, suggesting that little error could be attributed to vertical heterogeneity in CBL or tropospheric concentrations.

5.2. *Isotopic discrimination*

5.2.1. Carbon isotopes. Values obtained for $\Delta^{13}C$ ranged from 17‰ to 22‰, with the two budget methods agreeing well. These values correspond to a range of c_i/c_a from 0.6 to 0.8 (Table 3), and are comparable with other estimates for this biome in the literature. Global model estimates for boreal coniferous forests range from 15–17‰ (Lloyd and Farquhar 1994; Bakwin et al., 1998) to 20‰ (Fung et al., 1997, with seasonal amplitude ~1‰). Field measurements in a boreal pine forest found $\Delta^{13}C = 19$‰ (Flanagan et al., 1996). Leaf $\delta^{13}C$ at the study site was measured as −27 to −28‰ (PDB-CO_2), which with a mean CBL value of ∼ −7‰ (PDB-CO_2) implies an average $\Delta^{13}C$ of 20–21‰. It should be noted that these other estimates are all representative of the annual mean, while the study here represents only two days in the middle of the growing season.

Diurnal variation in $\Delta^{13}C$ would normally be expected to behave in a sense opposite to that observed, since stomatal conductance and c_i would be relatively high in the morning when vapour pressure deficit is low, leading to higher carbon isotope discrimination. The value estimated here for the morning of 24 July of 17‰ is lower than expected, and is perhaps affected by errors in the application of the CBL model, particularly in the incorporation of the residual boundary layer to the model, advective losses and/or vertical and horizontal heterogeneity in mixed-layer concentrations.

5.2.2. Oxygen isotopes. The estimates obtained for $\Delta^{18}O$ varied from around 40‰ for the afternoon periods to −5‰ for the morning period. Estimates from the two budget methods agreed reasonably well. With c_i/c_a calculated from $\Delta^{13}C$, c_c approximated by c_i and $\Delta^{18}O$ obtained from the CBL budget, the fractionation model described in section 2.4.2 can be used to determine δ_c and hence δ_s (Table 4). Due to the sandy soil in the pine forest area with low water-holding capacity, isotopic composition of source water should be close to that of recent precipitation, so the calculated value for δ_s could be used to validate the modelled oxygen isotope discrimination. Atmospheric vapour is assumed to be in isotopic equilibrium with source water, and e_a/e_i is equated to relative humidity as measured at the eddy covariance tower in the forest.

The last significant rainfall before the flights was three weeks earlier, and its isotopic composition was measured as −8‰ (versus the water isotopic standard SMOW). Composition of earlier rainfall ranged from −6‰ to −18‰ (SMOW). Soil evaporation between rain events would tend to enrich soil water composition. This would suggest that the estimates for source water of −7‰ and −10‰ (SMOW) for the afternoon periods of 23 and 24 July, respectively, were reasonable, whereas the values obtained for the intervening periods are overly depleted.

Concentration of CO_2 at the sites of carboxylation is likely to be lower than in the intercellular spaces (Evans and von Caemmerer, 1996); however a lower c_c results in an even more negative estimate of δ_s for

Table 4. *Ratio of intercellular to ambient CO_2 concentration (c_i/c_a) calculated from carbon isotope discrimination ($\Delta^{13}C$); and isotopic composition of chloroplast (δ_c) and source (δ_s) water calculated from oxygen isotope discrimination and ratio of ambient to intercellular vapour pressure (e_a/e_i)*[a]

Integration period	PM 23 Jul	Night + AM 23–24 Jul	AM 24 Jul	PM 24 Jul
$\Delta^{13}C$ (‰)	19.0	18.1	17.2	21.8
$\Delta^{18}O$ (‰)	37	−1	−5	43
c_i/c_a	0.65	0.61	0.57	0.77
e_a/e_i	0.36	0.52	0.47	0.43
δ_c (‰)	15	−6	−10	10
δ_s (‰)	−7	−23	−28	−10

[a]Isotope discriminations are those found using the integral CBL budget method with flask CO_2 data.

the night and morning periods. Similarly, a lower value of e_a/e_i should be used when weighted by assimilation rate, but this also reduces the estimated source water composition. Isotopic composition of chloroplast water is likely to be less enriched than the Craig–Gordon (CG) model predicts. Observations for bulk leaf water are indeed less enriched (Flanagan, 1993), and can be explained alternatively by the presence of several mixing pools (Yakir et al., 1989) or by opposing diffusion and convection from the sites of evaporation (the Péclet effect, Farquhar and Lloyd, 1993; see also review by Yakir, 1998 for discussion of various leaf water isotopic models). Wang et al. (1998) found that divergence of composition of chloroplast water from that predicted by the CG model increased with increasing Péclet number, but in contrast to other species, the single species of conifer they measured was well described by the CG model. Nevertheless, an isotopically heavier composition of water at the sites of evaporation than in chloroplast water, as found in most cases, implies a heavier value for source water, which may help to reconcile the results found here.

The CG model used here to estimate isotopic composition of water at the sites of evaporation applies to steady-state conditions only. Overnight it would be expected that chloroplast water would come close to equilibrating with source water, and it would take some time in the morning as the stomata open for the isotopic composition to move toward the steady-state CG value. Observations and model estimates by Cernusak et al. (2002) in Lupin suggest that, depending on the imbalance between transpiration and xylem flow, this effect can maintain leaf water compositions up to 5‰ below steady-state values. This disequilibrium could therefore be sufficient to maintain the depleted Siberian source water signature in the chloroplasts and produce the negative discriminations that were modelled for the morning period.

Another important process that may help to explain the apparent very negative source water composition is the possible covariance of c_i/c_a and chloroplast CO_2 isotopic composition (δ_c) between the forest and bog sites. Table 5 shows a simple calculation assuming much higher c_i and more negative δ_c in the bog compared to the forest. The oxygen isotope discrimination $\Delta^{18}O$ calculated for the aggregated bog and forest areas assuming an area ratio of 1:4 using the assigned values in Table 5 is the same as was found by the integral CBL budget calculation for the morning of 24 July (Table 3). It can be seen from Table 5 that the source water composition calculated from the aggregated discrimination is much more negative than that calculated for each of the bog and forest areas separately, using their individual values for δ_c and e_a/e_i. Calculation of aggregated carbon isotope discrimination $\Delta^{13}C$ with the assigned values for c_i/c_a in this example is also consistent with the value found by the ICBL budget method for AM 24 July (Table 3), but values for the bog and forest differ considerably. The example in Table 5 is exaggerated to illustrate the concept and discrimination was not assimilation-weighted, but assigned values are not beyond the range of possibilities. The inferred bog source water composition of −23‰ (SMOW) is still more negative than measured bog water values (−14‰, SMOW) and surrounding creeks (−18‰, SMOW), but is much closer than the estimate of −28‰ obtained from the aggregated data.

In other studies, diurnal variation in $\Delta^{18}O$ has been modelled from leaf water measurements to range from around −5‰ during the night and morning to 20‰ in the afternoon for a boreal pine forest with precipitation of similar isotopic composition (Flanagan et al., 1997), although humidity may not have been comparable to the present case. A global oxygen isotope discrimination model estimated $\Delta^{18}O$ as ~8‰ for the Zotino area based on a precipitation estimate of −18‰ (SMOW, Farquhar et al., 1993). The larger values found for the afternoon periods in this study (40–50‰) may indicate that the low humidity in the afternoons at the

Table 5. *Example calculation of the effect of aggregation of bog and forest areas when* c_i/c_a *and* δ_c *covary*

Area	c_i/c_a (assigned)	e_i/e_a (measured)	δ_c (assigned)	δ_s (calculated)	$\Delta^{18}O$ (calculated)	$\Delta^{13}C$ (calculated)
Bog	0.90	0.63	−10.0	−23.0	−73.0	24.7
Forest	0.48	0.46	4.0	−14.9	12.6	15.3
Forest + bog	0.56[a]	0.49[a]	−10.7[b]	−28.4[b]	−4.5[a]	17.2[a]

[a]Calculated as 0.2 × bog + 0.8 × forest.
[b]Calculated from aggregated $\Delta^{18}O$ value.

study site (∼40%) was producing greater evaporative enrichment of leaf water than was estimated or measured in the studies mentioned above.

5.3. Budget method comparison

The height integration method undertakes a straightforward mass difference approach, which relies only on the assumption of no advection and temporally constant concentration at the top of the integrating column. The ICBL budget method also assumes no advection, in addition to vertically constant concentration within the mixed layer (the CBL) and in the free troposphere (above the CBL).

The necessity of including subsidence and correcting for change in total air mass in the height integration method demonstrates over-simplification in the method. These corrections bring the method closer to the ICBL budget approach, where knowledge of boundary layer development is utilised to interpret changes in concentration over the day.

It was noted earlier that the height integration equation [eq. (5)] reduced to the ICBL budget equation [eq. (2), without the subsidence term] when the two layers corresponding to within and above CBL were chosen. In practice, however, there are factors complicating this equality, such as vertical contraction or expansion of the integrating column (the density correction), as well as variation of free tropospheric CO_2 concentration with time, which is not accounted for in the height integration method. If average free tropospheric concentrations are used between the two profiles over the integration period, then the two-layer height integration method [eq. (7), including density and subsidence corrections] agrees identically with the ICBL method [eq. (4)] except for the morning period on 24 July, where the treatment of the residual layer causes a slight difference between the methods (see discussion below). This suggests that the main deficiency in the height integration method is the assumption of time-invariant CO_2 concentrations at the top of the integrating column, and that this deficiency can perhaps be overcome by estimation of the rate of this change and appropriate correction. The data presented here suggest that the additional resolution of the multilayer height integration (more appropriate weighting of concentrations according to density at each level) does not significantly improve flux estimates, perhaps because the variation in concentrations with height within and, separately, above the CBL was reasonably small (Fig. 2).

The importance of the treatment of variation of free tropospheric concentrations in time is also evident in the ICBL budget method. Very different results are obtained when eq. (2) is used with the difference between above- and within-CBL concentrations for each profile independently ($c_{Bi} - c_{+i}$ at time t_i). This gives flux estimates of −1.6, −2.4, −7.2 and −0.5 μmol m^{-2} s^{-1} for the periods corresponding to PM 23 July, night + AM 23–24 July, AM 24 July and PM 24 July, respectively, in much poorer agreement with the eddy covariance measurements than when average free troposphere concentrations are used (eq. (4)]. The morning period of 24 July is not affected because the residual layer rather than the free troposphere is entrained during CBL growth.

The difference between the ICBL budget method and the two-layer height integration method when time-averaged tropospheric concentrations are used for the morning of 24 July can be determined from eqs. (4) and (7) as:

$$(F_{c,2HI} - F_{c,ICBL})_{\text{AM 24 July}} = \frac{(c_{RL} - \langle c_+ \rangle)(M_{B1} - M_{B0})}{T}$$

where 2HI refers to the two-layer height integration method; the subscript RL refers to the residual layer; and $M_{B0} = M_N + M_{RL}$, the sum of moles of air in the NBL and residual layer. This can be interpreted as accounting for the additional growth of the CBL beyond the height of the residual layer, where tropospheric concentrations are entrained. Recall that the treatment of the NBL and residual layer in the ICBL method for the morning of 24 July assumed no such additional entrainment. In this case, the height of the boundary layer in the afternoon was actually less than that of the residual layer in the morning by 50 m (Table 1). The principle applies equally well here because the whole of the residual layer would have been entrained into the growing boundary layer, rather than all but the last 50 m. This comparison has shown that it is important to take account of the evolution of the boundary layer beyond the point at which the residual layer is fully entrained. The ICBL budget may easily be rectified to include this contribution by adding the term shown in the equation above.

6. Conclusions

Two CBL budget methods were compared to infer average regional surface fluxes of CO_2 as well as carbon and oxygen isotope discrimination during CO_2 assimilation over a two-day period in July 1998 over a central Siberian forest and bog region.

CO_2 fluxes estimated from the integral CBL budget method [eq. (4)] agreed very well with eddy covariance flux measurements from the forest tower representing the dominant ecosystem type in the region. Estimates of $\Delta^{13}C$ for both afternoon periods were close to that expected from knowledge of C_3 plant carbon isotopic discrimination and measurements of leaf $\delta^{13}C$. Estimates of $\Delta^{18}O$ were more variable and hard to interpret without better knowledge of isotopic composition of plant leaf and source water, but may in part be explained by disequilibrium between chloroplast water and intercellular vapour, and by the contrasting influences of the two different ecosystem types in the region characterised by distinctive micrometeorology, transpiration and assimilation rates.

Applied in its simplest form, the height integration method [eq. (7)] was less successful than the ICBL budget method at predicting surface CO_2 fluxes and isotopic discrimination. A serious deficiency in the height integration method was shown to be in the assumption of constant scalar concentration at the top of the integrating column. Accounting for column density change, subsidence and time variation in free troposphere concentrations in the two-layer height integration method made it essentially identical to the ICBL method. Investigation of the differences between these two methods revealed that the ICBL method as applied to the morning period on 24 July had not properly accounted for the difference in height of the residual layer and the fully developed convective boundary layer. The magnitude of this term was quantified and may be incorporated into the ICBL budget equation for cases involving residual layers.

7. Acknowledgements

We thank Karl Kuebler for his technical assistance in the laboratory and field, Michael Raupach and Helen Cleugh for helpful discussions on interpretation of the data, and Jack Katzfey for supplying the relevant NCEP Reanalysis Project model data.

REFERENCES

Arneth, A., Kurbatova, J., Kolle, O., Shibistova, O. B., Lloyd, J., Vygodskaya, N. N. and Schulze, E.-D. 2002. Comparative ecosystem–atmosphere exchange of energy and mass in a European Russian and central Siberian bog II. Interseasonal and interannual variability of CO_2 fluxes. *Tellus* **54B**, this issue.

Bakwin, P. S., Tans, P. P., White, J. W. C. and Andres, R. J. 1998. Determination of the isotopic ($^{13}C/^{12}C$) discrimination by terrestrial biology from a global network of observations. *Global Biogeochem. Cycl.* **12**, 555–562.

Brutsaert, W. and Mawdsley, J. A. 1976. The applicability of planetary boundary layer theory to calculate regional evapotranspiration. *Water Resour. Res.* **12**, 852–857.

Cernusak, L. A., Pate, J. S. and Farquhar, G. D. 2002. Diurnal variation in the stable isotope composition of water and dry matter in fruiting *Lupinus augustifolius* under field conditions. *Plant, Cell and Environ.* (in press).

Cleugh, H. A. and Grimmond, C. S. B. 2001. Modelling regional scale surface energy exchanges and CBL growth in a heterogeneous, urban-rural landscape. *Boundary Layer Meteorol.* **98**, 1–31.

Craig, H. and Gordon, L. I. 1965. Deuterium and oxygen-18 variations in the ocean and marine atmosphere. In: *Proceedings of a Conference on Stable Isotopes in Oceanographic Studies and Palaeotemperatures* (ed. T. Tongiorgi). Laboratory of Geology and Nuclear Science, Spoleto, Italy, 9–130.

Denmead, O. T., Raupach, M. R., Dunin, F. X., Cleugh, H. A. and Leuning, R. 1996. Boundary layer budgets for regional estimates of scalar fluxes. *Global Change Biol.* **2**, 255–264.

Evans, J. R. and von Caemmerer, S. 1996. Carbon dioxide diffusion inside leaves. *Plant Physiol.* **110**, 339–346.

Farquhar, G. D. and Lloyd, J. 1993. Carbon and oxygen isotope effects in the exchange of carbon dioxide between terrestrial plants and the atmosphere. In: *Stable isotopes and plant carbon-water relations* (ed. J. R. Ehleringer, A. E. Hall and G. D. Farquhar). Academic Press, San Diego, 47–70.

Farquhar, G. D., O'Leary, M. H. and Berry, J. A. 1982. On the relationship between carbon isotope discrimination and the intercellular carbon dioxide concentration in leaves. *Aust. J. Plant Physiol.* **9**, 121–137.

Farquhar, G. D., Hubick, K. T., Condon, A. G. and Richards, R. A. 1989. Carbon isotope fractionation and plant water-use efficiency. In:, *Stable isotopes in ecological research* (ed. P. W. Rundel, J. R. Ehleringer and K. A. Nagy). Springer-Verlag, New York, 21–40.

Farquhar, G. D., Lloyd, J., Taylor, J. A., Flanagan, L. B., Syvertsen, J. P., Hubick, K. T., Wong, S. C. and Ehleringer, J. R. 1993. Vegetation effects on the isotope composition of oxygen in atmospheric CO_2. *Nature* **363**, 439–443.

Flanagan, L. B. 1993. Environmental and biological influences on the stable oxygen and hydrogen isotopic composition of leaf water. In: *Stable isotopes and plant* *carbon-water relations* (ed. J. R. Ehleringer, A. E. Hall and G. D. Farquhar). Academic Press, San Diego, 71–90.

Flanagan, L. B., Brooks, J. R., Varney, G. T., Berry, S. C. and Ehleringer, J. R. 1996. Carbon isotope discrimination during photosynthesis and the isotope ratio of respired CO_2 in boreal forest ecosystems. *Global Biogeochem. Cycles* **10**, 629–640.

Flanagan, L. B., Brooks, J. R., Varney, G. T. and Ehleringer, J. R. 1997. Discrimination against $C^{18}O^{16}O$ during photosynthesis and the oxygen isotope ratio of respired CO_2 in boreal forest ecosystems. *Global Biogeochem. Cycles* **11**, 83–98.

Fung, I., Field, C. B., Berry, J. A., Thompson, M. V., Randerson, J. T., Malmström, C. M., Vitousek, P. M., Collatz, G. J., Sellers, P. J., Randall, D. A., Denning, A. S., Badeck, F. and John, J. 1997. Carbon 13 exchanges between the atmosphere and biosphere. *Global Biogeochem. Cycles* **11**, 507–533.

Keeling, C. D. 1958. The concentrations and isotopic abundances of atmospheric carbon dioxide in rural areas. *Geochim. Cosmochim. Acta* **13**, 322–334.

Keeling, C. D. 1961. The concentrations and isotopic abundances of atmospheric carbon dioxide in rural and marine air. *Geochim. Cosmochim. Acta* **24**, 277–298.

Kurbatova, J., Arneth, A., Vygodskaya, N. N., Kolle, O., Varlagin, A. B., Milyukova, I. M., Tchebakova, N. M., Schulze, E.-D. and Lloyd, J. 2002. Comparative ecosystem-atmosphere exchange of energy and mass in a Europan Russian and a central Siberian bog I. Interseasonal and interannual variability of energy and latent heat fluxes during the snow-free period. *Tellus* **54B**, this issue.

Lloyd, J. and Farquhar, G. D. 1994. ^{13}C discrimination during CO_2 assimilation by the terrestrial biosphere. *Oecologia* **99**, 201–215.

Lloyd, J., Kruijt, B., Hollinger, D. Y., Grace, J., Francey, R. J., Wong, S.-C., Kelliher, F. M., Miranda, A. C., Farquhar, G. D., Gash, J. H. C., Vygodskaya, N. N., Wright, I. R., Miranda, H. S. and Schulze, E.-D. 1996. Vegetation effects on the isotopic composition of atmospheric CO_2 at local and regional scales: theoretical aspects and a comparison between rain forest in Amazonia and a boreal forest in Siberia. *Aust. J. Plant Physiol.* **23**, 371–399.

Lloyd, J., Francey, R. J., Sogachev, A., Byers, J. N., Kelliher, F. M., Mollicone, D., Raupach, M. R., Wong, S.-C., Arneth, A., Rebmann, C., Valentini, R. and Schulze, E.-D. 2001. Vertical profiles, boundary layer budgets, and regional flux estimates for CO_2 and its $^{13}C/^{12}C$ ratio and for water vapour above a forest/bog mosaic in central Siberia. *Global Biogeochem. Cycles* **15**, 267–284.

Lloyd, J., Shibistova, O., Tchebakova, N., Kolle, O., Arneth, A., Zolotoukhine, D., Styles, J. M. and Schulze, E.-D. 2002a. Seasonal and annual variations in the photosynthetic productivity and carbon balance of a central Siberian pine forest. *Tellus* **54B**, this issue.

Lloyd, J., Langenfelds, R. L., Francey, R. J., Gloor, M., Tchebakova, N. M., Zolotukhine, D., Brand, W. A., Werner, R. A., Jordan, A., Allison, C. A., Zrazhewske, V., Shibistova, O. and Schulze, E.-D. 2002b. A first trace gas climatology above Zotino, central Siberia. *Tellus* **54B**, this issue.

McNaughton, K. G. and Spriggs, T. W. 1986. A mixed-layer model for regional evaporation. *Boundary Layer Meteorol.* **34**, 243–262.

Miller, J. B., Yakir, D., White, J. W. C. and Tans, P. P. 1999. Measurement of $^{18}O/^{16}O$ in the soil-atmosphere CO_2 flux. *Global Biogeochem. Cycles* **13**, 761–774.

Munley, W. G. and Hipps, L. E. 1990. Estimation of regional evaporation for a tall grass prairie from measurements of properties of the atmospheric boundary layer. *Water Resour. Res.* **27**, 225–230.

O'Neill, J. R., Adami, L. H. and Epstein, S. 1975. Revised value for the O^{18} fractionation between CO_2 and H_2O at 25 °C. *J. Res. US Geol. Surv.* **3**, 623–624.

Raupach, M. R. 2000. Equilibrium evaporation and the convective boundary layer. *Boundary Layer Meteorol.* **96**, 107–141.

Raupach, M. R., Denmead, O. T. and Dunin, F. X. 1992. Challenges in linking atmospheric CO_2 concentrations to fluxes at local and regional scales. *Aust. J. Bot.* **40**, 697–716.

Shibistova, O., Lloyd, J., Evgrafova, S., Savushkina, N., Zrazhewskaya, G., Arneth, A., Knohl, A., Kolle, O. and Schulze, E.-D. 2002. Seasonal and spatial variability in soil CO_2 efflux rates for a central Siberian *Pinus sylvestris* forest. *Tellus* **54B**, this issue.

Stull, R. B. 1988. *An introduction to boundary layer meteorology*. Kluwer Academic Press, Norwell, 666 pp.

Tchebakova, N. M., Kolle, O., Zolotoukhine, D., Arneth, A., Styles, J. M., Vygodskaya, N. N., Schulze, E.-D., Shibistova, O. and Lloyd, J. 2002. Inter-annual and seasonal variations of energy and water vapour fluxes above a *Pinus sylvestris* forest in the Siberian middle taiga. *Tellus* **54B**, this issue.

Wang, X.-F., Yakir, D. and Avishai, M. 1998. Non-climatic variations in the oxygen isotopic compositions of plants. *Global Change Biol.* **4**, 835–849.

Wofsy, S. C., Harriss, R. C. and Kaplan, W. A. 1988. Carbon dioxide in the atmosphere over the Amazon basin. *J. Geophys. Res.* **93**, 1377–1387.

Yakir, D. 1998. Oxygen-18 of leaf water: a crossroad for plant-associated isotopic signals. In *Stable isotopes: integration of biological, ecological and geochemical processes* (ed. H. Griffiths). BIOS Scientific Publishers, Oxford, 147–168.

Yakir, D., De Niro, M. J. and Rundel, P. W. 1989. Isotopic inhomogeneity of leaf water: evidence and implications for the use of isotopic signals transduced by plants. *Geochim. Cosmochim. Acta* **53**, 2769–2773.